Simulated ion irradiation of (Bi, Pb)-2212 superconducting thin films for the creation of magnetic vortex pinning points

F.E. Sánchez-Zacate, C. Mejía García, E. Díaz Valdés

Ion irradiation over superconducting thin films of (Bi, Pb)-2212 ($Bi_{1.6}Pb_{0.4}Sr_2CaCu_2O_8$) were simulated using the software SRIM v.2013, to investigate effectiveness of this technique in creating magnetic vortices pinning points to increase the critical current density of the films. Irradiation of He, C, Si, Cu, Ag, or Au ions, with kinetic energies of 3 and 6 MeV, and angle of incidence of 0, 15, 30, 45, and 60 degrees, were simulated over films with thicknesses of 200, 500, and 1000 nm. Each atom displaced from its original position in the crystal lattice due to the fired ions was counted as a pinning point. Heavy ions such as Ag and Au were found to be the most efficient in creating pinning points. Ions with lower atomic mass like C, Si, and Cu produced a smaller number, but the sample is less likely to become amorphous due to the irradiation process. For a kinetic energy of 3 MeV, the quantity of ions trapped inside the film increases significantly, and it is only recommended for the thinnest films, or the lightest ions. A greater incidence angle increases the production of pinning points.

Introduction

Within the family of Bi-based superconductors, the compounds of the form $Bi_2Sr_2Ca_{n-1}Cu_nO_{2n+4}$ with n=1,2,3, show the highest superconducting transition temperatures (T_c). This kind of materials have a structure formed by blocks of SrO-BiO-BiO-SrO separated by blocks of CuO_2. The former serve as charge carrier reservoirs, while the quantity of layers in the copper oxide block is related to the T_c of the material. The compound Bi-2201 ($Bi_2Sr_2CuO_6$), with one single layer of CuO_2 in its crystalline structure, has the lowest T_c = 22 K. It is followed by Bi-2212 ($Bi_2Sr_2CaCu_2O_8$) with T_c = 80 K (two layers of CuO_2), and the Bi-2223 ($Bi_2Sr_2Ca_2Cu_3O_{10}$), with three layers of CuO_2, reaches the highest T_c = 110 K [1].

In practice, the synthesis of the above-mentioned superconducting phases results very complicated. Shortly after the discovery of this materials, it was found that the substitution of a quantity of Bi by Pb as part of the chemical precursors facilitates the formation of superconducting phases [2-4]. In this way, the compounds, (Bi, Pb)-2212 ($Bi_{1.6}Pb_{0.4}Sr_2CaCu_2O_8$) and (Bi, Pb)-2223 ($Bi_{1.6}Pb_{0.4}Sr_2Ca_2Cu_3O_{10}$), can be synthesized more easily, while keeping close superconducting properties respect to the compounds without Pb, for example, a similar T_c or a very high upper critical field (H_{c2}) [4-6].

Addition of Pb allows to carry out the synthesis and anneal processes of (Bi, Pb)-2212 films in an air atmosphere, in contrast to (Bi, Pb)-2223 phase, which requires a controlled atmosphere and a careful temperature control during long annealing processes [7-9]. Thus, the synthesis of (Bi, Pb)-2212 superconducting films can be performed using more accessible and cheaper techniques such as spray pyrolysis, in comparison to the sophisticated techniques required for (Bi, Pb)-2223. Furthermore, the T_c of (Bi, Pb)-2212 is over the boiling point of nitrogen, making it an interesting material for practical applications. For these reasons, the phase (Bi, Pb)-2212 was considered interesting and accessible to carry out a real experiment, and therefore, the computer simulations in this work were done for this compound.

Superconducting materials can support electrical currents four orders of magnitude greater than that of a copper wire. The critical current density (J_c) is the highest current that a superconductor can tolerate, however its theoretical limit is far from been reached. This limit called the depairing critical current density (J_D), is defined as the maximum current density that a superconducting material can carry before the Cooper pairs break into individual electrons [10]. At the present time, the difference between J_D and J_c values for any High-Critical Temperature Superconductor (HTS) is several orders of magnitude, so there is ample room for improvement.

A promising method to enhance J_c in a HTS is the ion irradiation. The objective is to create imperfections into the crystalline structure of the material, which serve as pinning points for the magnetic flux lines that emerge within a type II superconductor when it carries an electrical current [11,12]. As these magnetic vortices begin to move within the material, J_c rapidly decreases to zero. The creation of pinning points and the subsequent reduction in vortex mobility serve to enhance the magnitude of J_c of the film [13,14].

During irradiation, the incident ion has multiple collisions with the atoms forming the crystal lattice, on its way through the superconducting film. Each of these interactions transfer energy to the collided atoms through elastic collisions under the influence of a partially screened Coulomb potential [15,16]. However, for incident ions with kinetic energy of the order of MeV a good approximation with the simple Coulomb potential can be made [17]:

$$V(r) = \frac{1}{4\pi\epsilon_0}\frac{Z_1 e_1 Z_2 e_2}{r} \quad (1)$$

where Z_1 and Z_2 are the atomic numbers of the two particles

Francisco E. Sánchez-Zacate ✉, Concepción Mejía García, Elvia Díaz Valdés
Departamento de Física, Escuela Superior de Física y Matemáticas, Instituto Politécnico Nacional Gustavo A. Madero, Cd. Mex., 07738, México.

Presented at the *Theory and Simulations of Materials Simposium, XVII Intl. Conf. on Surfaces, Materials, and Vacuum, SMCTSM,* September 23rd to 27th, 2024. Ensenada, BC, Mexico.
Received: September 22nd, 2024.
Accepted: May 13th, 2025.
Published: May 31st, 2025.

https://doi.org/10.47566/2025_syv38_1-250502

involved in the collision, e_i is the elemental charge (1.60218×10^{-19} C) with positive or negative sign according to the particle, and ϵ_0 is the permittivity of free space (8.85418×10^{-12} $C^2/N \cdot m^2$). The energy transferred to the target depends on the initial energy of the projectile and the scattering angle of the collision. If it exceeds the displacement energy (E_d), then the collided atom will shift from its original position, generating a defect in the crystal lattice. The other mechanism by which the incident ion loses energy is the ionization (loss of electrons) of the target atom during the collision [15,16]. In this process the change in direction of the interacting particles is negligible. As it passes through the film, the incident ion creates a cascade of collisions. If its initial kinetic energy is large enough, it will pass through the film, otherwise it will be trapped within the crystal lattice.

In this work, computer simulations of ion irradiation over superconducting thin films of (Bi, Pb)-2212 ($Bi_{1.6}Pb_{0.4}Sr_2CaCu_2O_8$) were performed. Different types of ions and incidence angles were simulated for three different film thicknesses. The effect on the crystal lattice of the film was studied, in particular, the quantity of magnetic vortex pinning points created by the ion irradiation. The ultimate purpose of this work is to determine the optimal experimental conditions for conducting the actual experiment.

Experimental details

The ion irradiation over superconducting thin films of (Bi, Pb)-2212 was simulated using SRIM v. 2013 [18], this software uses the Monte Carlo method. The parameters of the superconducting films were: E_d = 25 eV, film thickness of δ = 1000, 500, and 200 nm, and a density $\rho_{(Bi,\ Pb)\text{-}2212}$ = 6.58 g/cm^3. To perform the simulations, six different ions covering a wide range of atomic masses were chosen: from light ions such as He and C, also Si and Cu, to heavy ions such as Ag and Au. This selection was made to study the effect of ion mass on the creation of vortex pinning points. Angle of incidence Θ = 0°, 15°, 30°, 45°, and 60°, with respect to the normal to the film surface. Initial kinetic energy of the incident ion E_k = 6 and 3 MeV. As mentioned before, the fired ions must completely pass through the film, to avoid the possible effects caused by the implantation of these ions inside the crystal lattice of the film. Thus, the simulations were performed with an initial kinetic energy of E_k = 3 MeV, with the purpose to minimize the number of ions trapped inside the films. Simulations were also performed with an energy of 6 MeV, which is the maximum kinetic energy that the particle accelerators available in Mexico can provide. For each selection of ion type, Θ, E_k, and film thickness, 100,000 fired ions were simulated (one at a time). Each atom displaced from its original place in the crystal lattice of the film by effect of the ion irradiation, was considered as the creation of a magnetic vortex pinning point. To estimate the average number of atoms displaced, it was selected the "quick calculation" option in SRIM, that uses the modified Kinchin-Pease model.

This model uses the concept of Primary Knock-on Atom (PKA), which is defined as the first atom that is displaced from its position in the crystal lattice as a result of the collision with the incident ion. If the energy transferred to this primary atom is large enough, it will collide with other atoms in the film, generating new displacements and creating a cascade of collisions. The modified Kinchin-Pease model makes the following assumptions [19, 20]:

i) The collisions occur between two particles.

ii) In practice, atoms are not impenetrable hard spheres. The model includes a factor (displacement efficiency) to compensate for the overestimation in the displacements counts due to the hard-sphere approximation.

iii) The probability that a collision produces the displacement of an atom of the crystal lattice is 0, if $E_i < E_d$, where E_i is the kinetic energy of the projectile. In case of $E_d < E_i < 2.5E_d$, the probability is 1.

iv) In case of $2.5E_d < E_i$, the probability to produce an atom displacement is $0.4\frac{E_i}{E_d}$.

v) In the range of MeV, the energy decreases through ionization and loss of electrons from the target atom, due to the collision with the incident ion.

Results and discussion

The computer simulations made allow to estimate the average number of vortices pinning points created per each type of ion passing through the target material. Figure 1a is the graph generated by SRIM. The shaded region in the horizontal plane shows the cumulative effect of the collision cascades generated by the one hundred thousand gold ions,

Table 1. Number of vortices pinning points (displacements) estimated in each simulation. E_k = 6 MeV. For example, using the simulation parameters: film thickness δ = 200 nm, Θ = 45 °, and a copper ion, it was estimated that each incident ion produces 747 displacements in the crystal lattice of the superconducting film.

δ (nm)		1000					500					200				
Θ (°)		0	15	30	45	60	0	15	30	45	60	0	15	30	45	60
Ion	**Z**	**Displacements per ion** (a.u.)														
He	2	2	1	2	2	3	1	1	1	1	1	0	0	0	0	0
C	6	43	46	52	70	122	19	20	24	29	44	7	7	9	10	15
Si	14	537	559	678	1027	2359	213	223	254	335	580	76	79	87	111	169
Cu	29	3409	3600	4369	6416	10563	1413	1468	1692	2260	4046	502	529	598	747	1136
Ag	47	10756	11397	13512	17919	23020	4488	4673	5398	7320	12170	1623	1689	1904	2418	3775
Au	79	31174	31503	32141	32405	32276	15196	15963	18472	23412	29181	5223	5413	6192	8046	12923

Table 2. Number of vortices pinning points (displacements) estimated in each simulation. E_k = 3 MeV.

δ (nm)		1000					500					200				
Θ (°)		0	15	30	45	60	0	15	30	45	60	0	15	30	45	60
Ion	**Z**	**Displacements per ion** (a.u.)														
He	2	3	3	4	4	6	1	1	1	2	3	0	0	0	1	1
C	6	98	105	123	192	494	39	42	47	60	106	14	14	16	21	31
Si	14	1200	1289	1660	2490	3318	412	431	507	720	1441	137	143	163	207	329
Cu	29	6943	7354	4369	10404	11637	2565	2733	3221	4505	7116	878	920	1036	1358	2232
Ag	47	16925	17150	17604	17877	17700	8003	8418	9821	12353	15273	2680	2810	3226	4241	6846
Au	79	19948	19947	19952	19936	19814	19059	19256	19647	19867	19810	7962	8284	9502	12097	16002

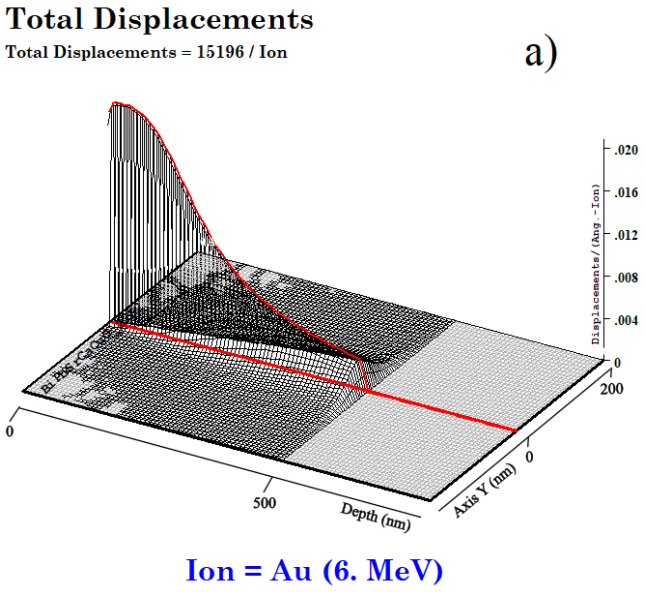

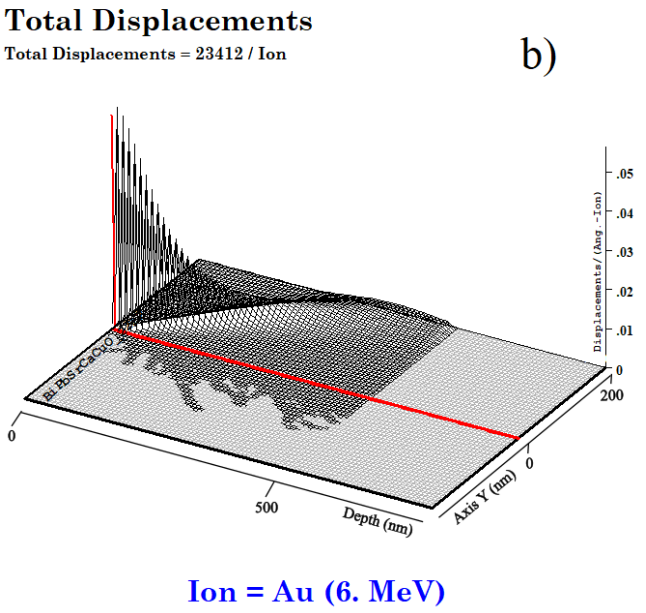

Figure 1. Effect of the collision cascades produce by the ion irradiation (shaded region in the horizontal plane). (Bi, Pb)-2212 films with δ = 500 nm. Au ions with E_k = 6 MeV. a) Θ = 0°. Curved red line: number of atom displacements in relation to the depth within the film. On average, each incident ion generated 15196 displacements (pinning points). b) The angle Θ = 45° directs the growth of the collision cascades. There is an increase in the number of displacements produced, 23412.

fired (one by one) on the thin film with E_k = 6 MeV, and Θ = 0°. Then, in this case, the fired ions have a direction parallel to the red straight line. It can be seen how the first interactions between the fired ion and the film rapidly creates a cascade of collisions across the film. The top of the curved red line indicates that more displacements (pinning points) are generated near the film surface, and this production decreases as the ion loses energy on its way through the film. Likewise, Figure 1b shows the result for E_k = 6 MeV and Θ = 45°: the angle directs the growth of the collision cascades, and there is also an increase in the number of displacements produced by each incident ion. Similar graphs were obtained using the different simulation parameters.

Table 1 shows the results obtained from all simulations with E_k = 6 MeV for different film thicknesses, angle Θ, type of ion and atomic number (Z). Table 2 have similar results for E_k = 3 MeV. The number of displacements is the average obtained from the one hundred thousand iterations in a single simulation. Only the creation of vacancies was counted as displacements, collisions of ions with energy $E_i < E_d$ were not counted by SRIM, because generates a temporary shift in the position of the atom hit, which then returns to its original site in the crystal lattice. As can be seen in both tables, heavy ions (Au and Ag) generate the largest number of pinning points for a given angle Θ. In contrast, He ions have an almost null production of displacements, regardless of Θ or E_k, and can therefore be discarded for use in creating pinning points to increase the J_c of the superconducting films.

As the atomic number (Z) of the incident ion increases, the number of pinning points (displacements) grows rapidly. This can be explained as follows; In an elastic collision, the energy transferred to the target (E_T) depends on the masses of the projectile (M_1) and the target (M_2), in addition to the scattering angle (φ) and the initial kinetic energy E_i of the projectile [16,21]:

$$E_T = \frac{4M_1M_2}{(M_1+M_2)^2} \cdot cos^2(\varphi) \cdot E_i \qquad (2).$$

Therefore, a projectile of greater mass transfers more energy to the collided atom of the crystal lattice, increasing the probability to generate a permanent position shift of that atom. However, in the same way, a heavier ion exhausts its kinetic energy ahead. This can be seen in the plots corresponding to δ = 1000 nm of Figure 2a, and also in the plots of δ = 1000 and 500 nm of Figure 2b; In both graphs it is observed that although the absolute maximum in the

number of displacements is produced by the Au ion with $\Theta = 60°$, this value is practically reached since smaller angles. In Figure 2a ($E_k = 6$ MeV), the mentioned plots tend to a maximum around 32276 displacements, for any angle Θ. This is because after a certain number of collisions, the heavy ion has exhausted its kinetic energy, and thus, a lengthening of the trajectory due to a wider angle Θ no longer increases the number of displacements produced. In the case of Figure 2b ($E_k = 3$ MeV), the plots ($\delta = 1000$, 500 nm) tend to a maximum around 19814 displacements, regardless of the film thickness or the angle Θ, but the depletion of the kinetic energy is evident since the Ag ion.

The number of displacements increases quadratically with respect to the value of Z of the incident ion; the curves in Figure 2a ($E_k = 6$ MeV) can be fitted to a square power, for example, the pink curve with parameters $\delta = 1000$ nm and $\Theta = 0°$, fits well to equation $Y = 5.55X^2$, $R^2 = 0.99$. The exception are the plots corresponding to $\delta = 1000$ nm, with $\Theta = 45°$, 60°; these first grow rapidly and later has a drop in the displacement production trend for the ion of gold. In Figure 2b ($E_k = 3$ MeV), the drop in the displacement production begins in the curve with $\delta = 500$ nm and $\Theta = 45°$, which starts not fitting well to a square power: $Y = 3.48X^2$, $R^2 = 0.9$. Thus, the optimal utilization of E_k is achieved in this last curve (red triangle) for the ion of gold; by doubling the thickness of the film or increasing Θ, virtually the same number of pinning points are still created.

In Figure 2a, it can also be observed that for the film with $\delta = 500$ nm and $\Theta = 60°$, the number of pinning points created outperforms the results obtained for small values of Θ in films with $\delta = 1000$ nm irradiated with Ag ions. A wider

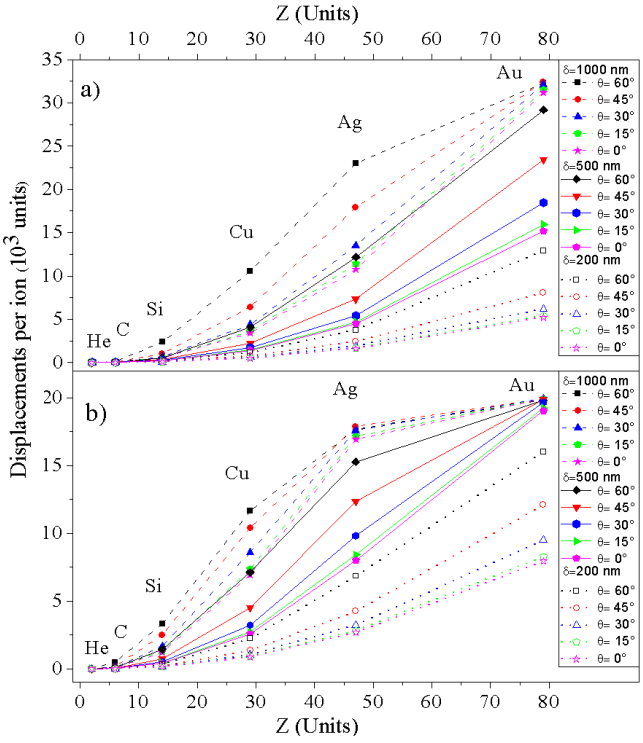

Figure 2. Displacements per ion vs Atomic number Z. The lines are guides for the eyes. Dashed lines: $\delta = 1000$ nm. Solid lines: $\delta = 500$ nm. Dotted lines $\delta = 200$ nm. a) $E_k = 6$ MeV. b) $E_k = 3$ MeV.

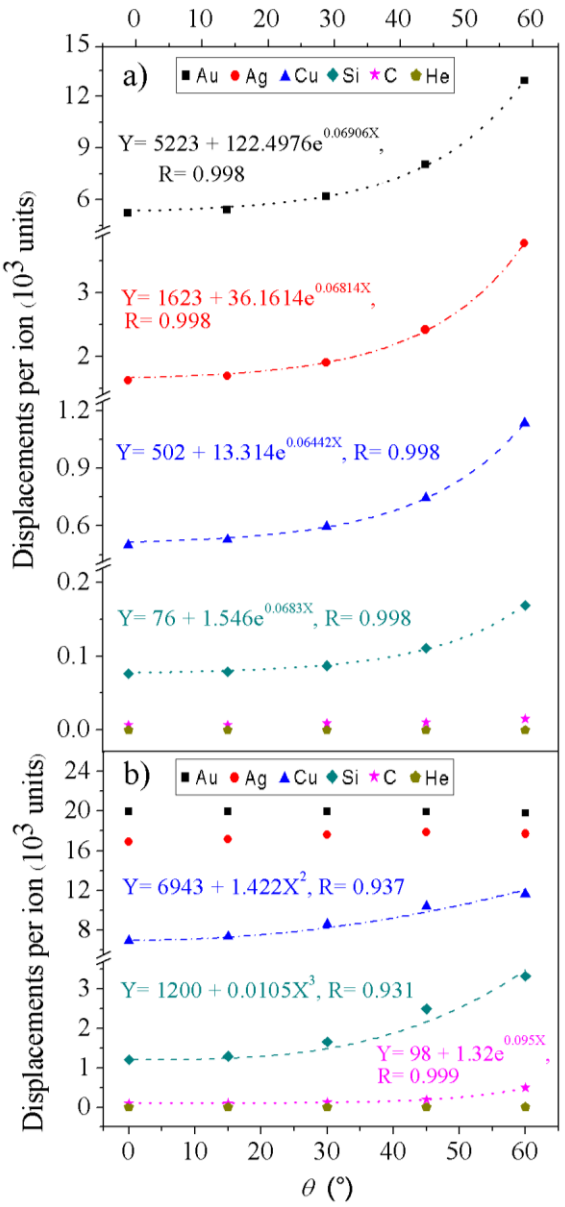

Figure 3. Displacements per ion vs Angle of incidence Θ. The lines indicate the corresponding least squares fit. a) Ions with $E_k = 6$ MeV, and films with $\delta = 200$ nm. b) Ions with $E_k = 3$ MeV, and films with $\delta = 1000$ nm.

angle Θ, extends the trajectory of the projectile through the film. For most of the ion types, a longer path length results in more collisions, and therefore, a higher number of pinning points created. For example, Figure 3a shows the graphs of the Displacements per ion vs Angle of incidence Θ, for ion irradiation with $E_k = 6$ MeV, and films with $\delta = 200$ nm. For ions of Si and heavier than this, it is observed that the number of pinning points created has an exponential dependence on the angle Θ. However, there are exceptions; lighter ions, like He and C, do not show a great augment in the number of pinning points created by increasing Θ. In counterpart, the Figure 3b shows similar graphs for $E_k = 3$ MeV and $\delta = 1000$ nm, where the depletion of energy is already observed for most ions. In principle, the plot for the C ion can be fitted to an exponential function, but this is no longer true for the Si plot, which shows a cubic behavior. The

growth ratio decreases as a function Θ, the plot for the Cu ion shows a quadratic dependence on Θ, and finally for the ions of Ag and Au, the number of pinning points created practically does not increase for larger values of Θ.

Regarding the quantity of transmitted ions, that is, how many of them completely pass through the film structure, it was found that for E_k = 3 MeV, the Au ions are mostly trapped within all the films, except for δ = 200 and $\Theta \leq 30°$. With more energy (E_k = 6 MeV), they can pass through films of δ ≤ 500 nm and $\Theta \leq 30°$, with less than 20% of trapped ions. In a similar way, Ag ions with E_k = 3 MeV can pass through films of δ = 500 nm and $\Theta \leq 15°$, and for E_k = 6 MeV, films up to δ = 1000 nm and $\Theta \leq 30°$. This is important because ions trapped inside the crystalline structure can modify the superconducting properties of the film [22,23]. The lightest ions were able to pass through almost all films with less than 20% of ions trapped, even for E_k = 3 MeV; in the case of Si ions, films of δ = 1000 nm and $\Theta \leq 30°$. And for C ions, $\Theta \leq 45°$.

Conclusions

Based on the simulations made in this work, it was found that irradiation with heavy ions such as Au and Ag, are the most effective for the creation of magnetic vortices pinning points that formed inside the type II superconductors like (Bi, Pb)-2212, and thus increase the J_c of the superconducting films. However, these ions require a higher kinetic energy (E_k = 6 MeV) to not being trapped within the crystalline structure of the film, which would alter its superconducting properties. Lighter ions such as Cu, Si or C create a smaller quantity of pinning points, but their use is not discarded, since this lower efficiency also implies less damage to the film structure, i.e., less amorphization. Therefore, irradiation with these ions is appropriate to be applied to materials where heavy ions would result destructive. A kinetic energy of 3 MeV could only be used in films with a thickness of 200 nm or with light ions such as Si or C, to prevent trapping of the fired ions. A greater incidence angle of the irradiated ions allows to increase the number of pinning points produced. This is useful, as long as the kinetic energy of the ion is not exhausted, since in such a case the number of trapped ions also increases. The results presented here serve as a reference for the experimental conditions necessary to perform ion irradiation of (Bi, Pb)-2212 superconducting films in a real experiment.

Acknowledgements

F. E. Sánchez-Zacate expresses his gratitude to the SECIHTI (formerly CONAHCYT) of Mexico for the postdoctoral fellowship received to realize a research stay at Escuela Superior de Física y Matemáticas of the Instituto Politécnico Nacional, in Mexico City, from October 2022 to September 2025. This work is sponsored in part by the Secretaría de Investigación y Posgrado of Instituto Politécnico Nacional, under projects SIP 20250122 and SIP 20242201.

References

[1]. S. Nhien, G. Desgardin, *Phys. C* **272**, 309 (1996).
[2]. A. Kikuchi, M. Matsuda, M. Takata, M. Ishii, T. Yamashita, H. Koinuma, *Jpn. J. Appl. Phys*. **27**, L2300 (1988).
[3]. A. Jeremie, K. Alami-Yadri, J.-C. Grivel, R. Flükiger, *Supercond. Sci. Technol.* **6**, 730 (1993).
[4]. H. Raffy, J. Arabski, A. Vaurès, *J. Less-Common Metals* **151**, 385 (1989).
[5]. M. Matsuda, Y. Iwai, M. Takata, M. Ishii, T. Yamashita, H. Koinuma, *Jpn. J. Appl. Phys*. **27**, L1650 (1988).
[6]. L. Zhang, J.Z. Liu, R.N. Shelton, *Phys. Rev. B* **45**, 4978 (1992).
[7]. A. Sajjadi, I.W. Boyd, *Appl. Phys. Lett.* **63**, 3373 (1993).
[8]. D.K. Walia, A.K. Gupta, G.S.N. Reddy, V.S. Tomar, N.D. Kataria, V.N. Ojha, N. Khare, *Solid State Commun.* **71**, 987 (1989).
[9]. S. Turkoglu, M.A. Aksan, *J. Supercond. Nov. Magn.* **25**, 2087 (2012).
[10]. B. Shabbir, X. Wang, Y. Ma, S.X. Dou, S.S. Yan, L.M. Mei, *Sci. Rep.* **6**, 23044 (2016).
[11]. D. X. Huang, Y. Sasaki, S. Okayasu, T. Aruga, K. Hojou, Y. Ikuhara, *Phys. Rev. B* **57**, 13907 (1998).
[12]. F.M. Sauerzopf, *Phys. Rev. B* **57**, 10959 (1998).
[13]. H. Matsui, H. Ogiso, H. Yamasaki, T. Kumagai, M. Sohma, I. Yamaguchi, T. Manabe, *Appl. Phys. Lett*. **101**, 232601 (2012).
[14]. L. Fang, Y. Jia, V. Mishra, C. Chaparro, V.K. Vlasko-Vlasov, A.E. Koshelev, U. Welp, G.W. Crabtree, S. Zhu, N.D. Zhigadlo, S. Katrych, J. Karpinski, W.K. Kwok, *Nat. Commun.* **4**, 2655 (2013).
[15]. W.J. Weber, D.M. Duffy, L. Thomé, Y. Zhang, *Curr. Opin. Solid State Mater. Sci.* **19**, 1 (2015).
[16]. M. Backman, *Effects of nuclear and electronic stopping power on ion irradiation of silicon-based compounds, PhD Dissertation* (University of Helsinki, 2012).
[17]. B. Rauschenbach, *Low-Energy Ion Irradiation of Materials*, 1st ed. (Springer International Publishing, 2022) p. 10-12.
[18]. J.F. Ziegler, M.D. Ziegler, J.P. Biersack, *Nucl. Inst. Methods Phys. Res. B* **268**, 1818 (2010).
[19]. G.H. Kinchin, R.S. Pease, *Rep. Prog. Phys.* **18**, 1 (1955).
[20]. M.J. Norgett, M.T. Robinson, I.M. Torrens, *Nucl. Eng. Des.* **33**, 50 (1975).
[21]. B. Rauschenbach, *Low-Energy Ion Irradiation of Materials*. 1st ed. (Springer International Publishing, 2022) p. 21-22.
[22]. B.A. Young, J.R. Williams, S.W. Deiker, S.T. Ruggiero, B. Cabrera, *Nucl. Inst. Methods Phys. Res. A* **520**, 307 (2004).
[23]. M. Oh, J. Lee, W. Kang, S. Lee, Y. Jo, *APL Mater.* **12**, 031120 (2024).

The results included in this article were presented at the *Theory and Simulations of Materials Simposium, of the XVII International Conference on Surfaces, Materials, and Vacuum, SMCTSM*, September 23rd to 27th, 2024. Ensenada, BC, Mexico. (see Editorial Note https://doi.org/10.47566/2024_syv37_0-240001).